

# Supporting Information

Sandberg et al. 10.1073/pnas.1001740107

## SI Materials and Methods

**Molecular Modeling.** Modeling was carried out using PyMol (DeLano Scientific) and Swiss-PdbViewer ([www.expasy.org/spdbv](http://www.expasy.org/spdbv)) with a Gromos96 force field (1).

**Peptide Production and Purification.** The bacterial expression vector pACYCDuet-1 (Novagen) carrying the genes for the histidine-tagged Affibody ZA $\beta$ 3 and the wild-type A $\beta$  peptide has been described previously (2). The Ala21Cys and Ala30Cys mutations in A $\beta$ <sub>40</sub> and A $\beta$ <sub>42</sub> were introduced using the QuikChange kit for site directed mutagenesis (Stratagene) and confirmed by sequencing. *Escherichia coli* BL21(DE3) cells (Novagen) were transformed with the mutated expression vector and grown at 37 °C in Terrific Broth medium supplemented with 34  $\mu$ g mL<sup>-1</sup> chloramphenicol. When the optical density at 600 nm reached 0.8, expression was induced by the addition of 1 mM isopropyl- $\beta$ -D-1-thiogalactopyranoside (IPTG). Cells were harvested after 4 h and washed once with ice-cold Tris buffer (20 mM Tris, 50 mM NaCl at pH 8.5). Cell pellets were stored at -20 °C.

Upon use, cells were thawed and resuspended in Tris buffer supplemented with 5% glycerol, 0.5% Triton X-100, 1 mM phenylmethylsulphonyl fluoride (PMSF), and a few grains of DNase. Lysis of the cells was commenced using freeze-thaw cycles (typically five) and finalized by sonication following standard procedures. Lysed cells were centrifuged at 20,000  $\times$ g for 40 min at 4 °C, and the supernatant was subjected to immobilized metal affinity chromatography (IMAC) using Ni-NTA resin (Sigma). IMAC purifies the histidine-tagged Affibody and, hence, also the Affibody-A $\beta$ cc complex. The eluted fraction containing protein was immediately made 5 to 10 mM EDTA and stored on ice.

IMAC-purified Affibody and Affibody-A $\beta$ cc complex were concentrated using VIVASPIN 20 spin columns with a molecular weight cutoff of 3,000 Da (Sartorius) at 3,500  $\times$ g and 4 °C. The concentrated solution was subjected to size exclusion chromatography (SEC) using either a Superdex 200 or a Superdex 75 16/60 column (GE Healthcare) in Tris buffer supplemented with an additional 50 mM of NaCl (total, 100 mM NaCl). Occasionally, phosphate buffer (50 mM potassium phosphate, 50 mM NaCl at pH 7.2) was used in this step with no change in SEC performance. The fractions corresponding to the Affibody-A $\beta$ cc complex were pooled, and the complex was dissociated by the addition of solid guanidinium chloride (GdmCl) to a concentration of 6 to 7 M.

The Affibody was removed from the solution by IMAC under denaturing conditions in Tris or phosphate buffer supplemented with 6 to 7 M GdmCl. The flow-through contains A $\beta$ cc in denaturing buffer, which keeps it soluble. This solution was concentrated using spin columns as above and subjected to SEC equilibrated with phosphate buffer, the corresponding buffer made from the sodium phosphate salt, or phosphate buffer with sodium fluoride instead of sodium chloride [for circular dichroism (CD) measurements]. On the SEC column, the peptide is subjected to native conditions and starts aggregating into oligomers, as described in the main text. The SEC fractions of the different oligomeric species were pooled separately and concentrated using spin columns as described above. SEC columns used in this study were all prepacked by the manufacturer, and include Superdex 75 PG 16/60 and HR 10/300, Superdex 200 PG 16/60 and HR 10/300, and Sephacryl 300 HR 26/60 columns (all from GE Healthcare).

The concentration of purified A $\beta$ cc peptides was determined using an extinction coefficient of 2,230 M<sup>-1</sup> cm<sup>-1</sup> for the difference in absorbance at 280 and 300 nm. Yields were typically on the order of 2.5 to 4 mg L<sup>-1</sup> culture. Purified peptides were

either used immediately or stored at -80 °C. Frozen samples remain indistinguishable from unfrozen samples with respect to biophysical, cell biological, and immunological characteristics. However, no samples used in this study were frozen and thawed more than once.

Wild-type A $\beta$ <sub>40</sub> and A $\beta$ <sub>42</sub> were produced in the same way, except for mAb158 ELISA and neurotoxicity measurements.

**SDS/PAGE.** SDS/PAGE was carried out using the Criterion Gel system and precast 16.5% Tris-tricine gels (Bio-Rad) operated at a constant voltage of 120 V. The running buffer was 100 mM Tris-HCl, 100 mM tricine, and 0.1% SDS (pH 8.3). Approximately 2 to 7  $\mu$ g A $\beta$  peptides was diluted in 15  $\mu$ L phosphate buffer and mixed with equal parts loading buffer containing 50 mM Tris-HCl, 1% SDS, 20% glycerol, 0.23% bromophenol blue, and 2.5 mM (heat-stable) TCEP (Tris-2-carboxyethyl-phosphine) reducing agent. Samples were then heated at 95 °C for 5 min. Thirty microliters were then loaded in each well. Gels were stained by Coomassie.

**Fibril Formation Assays.** Formation of amyloid fibrils was followed by monitoring the fluorescence of thioflavin T (ThT) using a FLUOstar Optima reader (BMG) equipped with 440-nm excitation and 480-nm emission filters. The assay was carried out at 37 °C in 96-well plates (Nunc) sealed with polyolefin tape (Nunc) to prevent evaporation. Two minutes of orbital shaking (width 5 mm) preceded the measurement of each datapoint at an interval of 6 min. Alternatively, when datapoints were collected at an interval of 15 min, 5 min of orbital shaking preceded each measurement. Phosphate buffer supplemented with 10  $\mu$ M ThT was used throughout. The stabilizing Cys21-Cys30 disulfide in A $\beta$ cc was reduced by the addition of 5 to 20 mM TCEP to the reaction mixture.

**Circular Dichroism.** CD was recorded on a Jasco J-810 spectropolarimeter (Jasco Corporation) at 20 °C. Diluted phosphate buffer or an equivalent buffer with sodium fluoride instead of sodium chloride was used in all CD measurements, which were carried out using 1-mm or 0.1-mm cuvettes cells. Secondary-structure content was estimated using the dichroweb server at <http://dichroweb.cryst.bbk.ac.uk> (3).

**Infrared Spectroscopy.** Fourier transform infrared (FTIR) spectra were recorded at 4 cm<sup>-1</sup> resolution on a Vertex 70 FTIR spectrometer (Bruker Optik GmbH) equipped with an HgCdTe detector and an ATR (attenuated total reflection) crystal. The experiments were performed at room temperature on 2  $\mu$ L of 0.6-mM A $\beta$ <sub>42</sub>CC samples that had been dried on an ATR crystal with nitrogen gas. Two experiments of 150 scans each were recorded and averaged and a 500-scan single-beam background spectrum was subtracted. The amide I band was deconvoluted by subtracting a linear baseline and spectral components were identified as second derivative minima. Gaussian functions centered at the corresponding positions were then fitted to the spectrum by optimizing intensities and line widths using software provided by the instrument manufacturer.

**Transmission Electron Microscopy.** Transmission electron microscopy (TEM) was measured on a LEO 912 AB OMEGA electron microscope (Carl Zeiss SMT AG) equipped with a Mega View CCD camera (Olympus). Negative staining with uranyl acetate was used in all samples. Formvar/carbon coated nickel grids were activated with UV light for 5 min, after which 5 to 10  $\mu$ L of protein

sample was applied to each grid for 2 min. Two steps of washing with 10  $\mu\text{L}$  of filtered deionized  $\text{H}_2\text{O}$  preceded the staining. A 2-min treatment with 2% uranyl acetate solution in filtered deionized  $\text{H}_2\text{O}$  completed the preparation of the grids, which were allowed to air dry for a few minutes before storage or analysis.

**Atomic Force Microscopy.** Atomic force microscopy (AFM) images were acquired with a Molecular Imaging PicoPlus setup using MikroMasch NSC36 silicon cantilevers.  $\text{A}\beta_{42}$  aliquots at  $\sim 50\text{-}\mu\text{M}$  concentrations in phosphate buffer were diluted by a factor of 5 to 40 in deionized water, deposited onto freshly cleaved mica substrates (Agar Scientific), and left to dry in air. The dried sample was finally rinsed with 50  $\mu\text{L}$  of deionized water to remove residual salt from the surface; after the surface was dry anew, images were acquired in air in intermittent contact mode.

**mAb158 ELISA.** Ninety-six-well EIA/RIA plates (Corning) were coated by overnight incubation at 4  $^\circ\text{C}$  with 2  $\mu\text{g}/\text{mL}$  mAb158 antibody in PBS. Plates were blocked with 1% BSA (BSA) in PBS with 0.15% Kathon preservative (Rohm and Haas) at pH 7.4 for 2 h at 37  $^\circ\text{C}$  before adding duplicates of  $\text{A}\beta_{42}$ , serially diluted in ELISA incubation buffer containing 0.05% Tween 20, 0.1% BSA, and 0.15% Kathon in PBS at pH 7.4. Synthetic wild-type  $\text{A}\beta_{42}$  protofibrils (4) ranging from 1 nM and down to low pM concentrations were used as positive control and wells coated with only ELISA incubation buffer were used as negative control. Samples were incubated for 2 h at 37  $^\circ\text{C}$ , 0.5  $\mu\text{g}/\text{mL}$  biotinylated mAb158 was added, and plates were incubated 1 h at 37  $^\circ\text{C}$  followed by incubation for 1 h at 37  $^\circ\text{C}$  with streptavidin-coupled horseradish peroxidase (HRP; Mabtech AB). K-blue enhanced (ANL Produkter) was used as HRP substrate and the reaction was stopped using 2 M  $\text{H}_2\text{SO}_4$ . Plates were read by a SpectraMAX 190 (Molecular Devices) spectrophotometer at 450 nm and 650 nm. After blocking, wells were washed three times with ELISA washing buffer (phosphate buffered NaCl with 0.1% Tween 20 and 0.15% Kathon) between each step of the ELISA. Differences in measured optical density in duplicate samples are typically less than 1%.

**A11 Dot Blot.** The anti- $\text{A}\beta$  oligomer serum A11 (Biosource) was used at a concentration of 0.5  $\mu\text{g mL}^{-1}$  according to the manufacturer's instructions. Polyvinylidene fluoride (PVDF) Immobilon-FL or Immobilon-PSQ membranes (Millipore) were used throughout. Samples were normalized with respect to the amount loaded and 5 to 10  $\mu\text{L}$  of each sample was applied onto untreated membranes and allowed to dry. A HRP-conjugated goat anti-rabbit IgG antibody (Zymed Laboratories) was used to detect bound A11 antibodies using a CCD camera and SuperSignal West Pico (Thermo Scientific) as substrate.

**Neurotoxicity Assays.** SHSY-5Y human neuroblastoma cells were cultured in a 96-well plate in a 50:50% mixture of DMEM:F12-Ham's Medium supplemented with 10% vol/vol FBS (Sigma). After 24 h in culture, the cell medium was removed and replaced with serum-free medium.  $\text{A}\beta_{42}$  monomer or oligomer fractions from SEC, which had been concentrated to  $\sim 75$  to 250  $\mu\text{M}$  in phosphate buffer without potassium (50 mM sodium phosphate, 50 mM NaCl at pH 7.2), were added to cell cultures to achieve final concentrations of 10, 5, or 1  $\mu\text{M}$ . Wild-type and  $\text{A}\beta_{42}\text{E22G}$  peptides (Bachem) were prepared as described previously (5) and resuspended to a final concentration of 50  $\mu\text{M}$  in sterile PBS. Wild-type  $\text{A}\beta$  and  $\text{A}\beta_{42}\text{E22G}$  fibrils were prepared by agitating the monomer solutions on an orbital eppendorf shaker 600 rpm for 2 h at 37  $^\circ\text{C}$ , which we have shown previously is sufficient to achieve fibril formation (5). Wild-type  $\text{A}\beta$  oligomers were prepared by diluting peptides dissolved in DMSO at 5 mM into PBS at 100  $\mu\text{M}$  concentration and letting the samples age without agitation into oligomers for 24 h at 4  $^\circ\text{C}$  (6). Untreated cells were cultured in serum-free medium diluted with sterile PBS to achieve the same final concentration of medium components as in the peptide-treated wells.

Caspase activity in each well was measured after 24 h of incubation using a Caspase-3/-7 fluorescence assay (Promega) and a plate reader (Fluostar Optima, BMG Labtech). Each treatment was performed in triplicate and differences between treatment conditions were assessed by ANOVA and post hoc *t* tests.

1. Scott WRP, et al. (1999) The GROMOS biomolecular simulation program package. *J Phys Chem A* 103:3596–3607.
2. Macao B, et al. (2008) Recombinant amyloid beta-peptide production by coexpression with an affibody ligand. *BMC Biotechnol* 8:82.
3. Whitmore L, Wallace BA (2008) Protein secondary structure analyses from circular dichroism spectroscopy: Methods and reference databases. *Biopolymers* 89:392–400.

4. Englund H, et al. (2007) Sensitive ELISA detection of amyloid-beta protofibrils in biological samples. *J Neurochem* 103:334–345.
5. Luheshi LM, et al. (2007) Systematic in vivo analysis of the intrinsic determinants of amyloid  $\beta$  pathogenicity. *PLoS Biol* 5:e290.
6. Lambert MP, et al. (1998) Diffusible, nonfibrillar ligands derived from  $\text{A}\beta_{1-42}$  are potent central nervous system neurotoxins. *Proc Natl Acad Sci USA* 95:6448–6453.

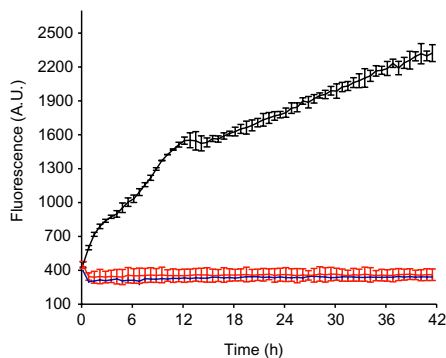


**Fig. S1.** ThT fluorescence assays of aggregation of 100  $\mu\text{M}$   $\text{A}\beta_{42}\text{CC}$  from the 100 kDa ( $\beta$ -sheet oligomer) SEC fraction in the absence (red) and presence (black) of 20 mM TCEP. Blue: baseline. See also Fig. S6C, which shows that amyloid fibrils do not form, even after days at 37  $^\circ\text{C}$ , but that amorphous A11-binding aggregates instead eventually form in samples of monomeric  $\text{A}\beta_{42}\text{CC}$ .

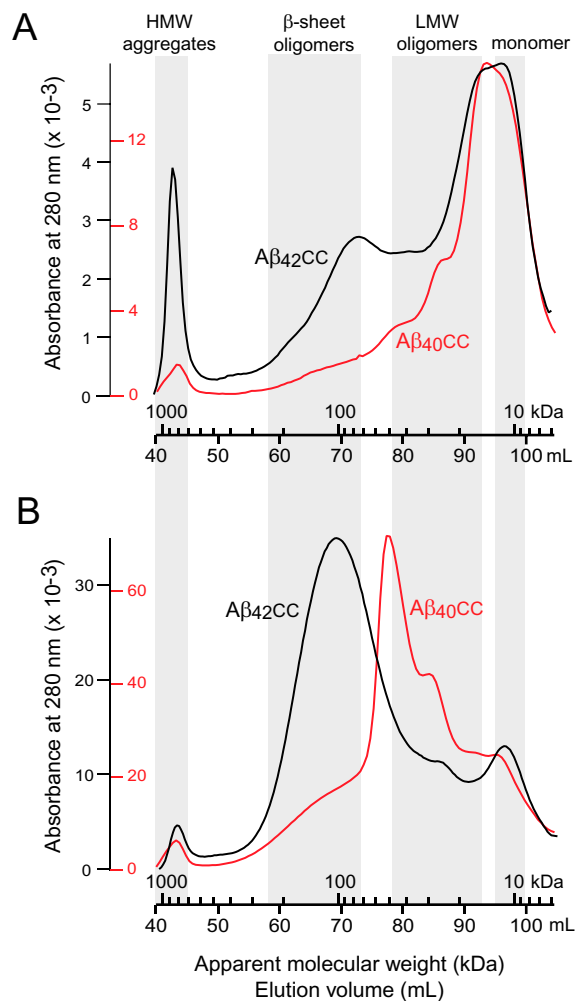


**Fig. S2.** Concentration dependence of formation of  $A\beta_{cc}$  oligomers from denatured  $A\beta_{cc}$  during SEC in native buffer on a Superdex 200 PG 16/60 column. (A) Diluted and (B) ~5 times more concentrated  $A\beta_{40CC}$  and  $A\beta_{42CC}$  samples. The experiments in B are the same as in A. Monomer peptide samples were loaded in denaturing buffer containing 7 M GdmCl and eluted with native phosphate buffer at pH 7.2, resulting in oligomer formation. Shaded zones indicate approximate elution volumes for different aggregates. The column was calibrated using globular protein standards. Sample amounts: (A) 0.5 mg  $A\beta_{40CC}$  and 0.3 mg  $A\beta_{42CC}$ ; (B) 2.7 mg  $A\beta_{40CC}$  and 1.7 mg  $A\beta_{42CC}$ .

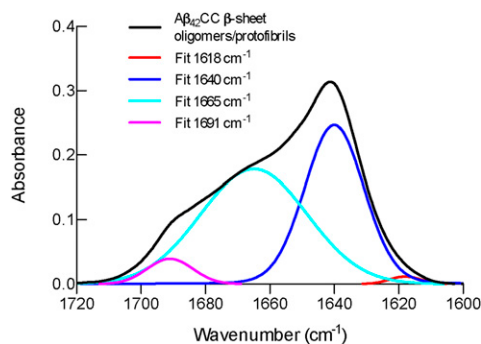


**Fig. S3.** FTIR spectroscopy of dried  $\beta$ -sheet oligomers/protofibrils of  $A\beta_{42CC}$ . The amide I band of the IR spectrum (black) was deconvoluted based on observed second-derivative minima, as indicated. The presence of an absorption peak at  $\sim 1,691\text{ cm}^{-1}$  is a hallmark of antiparallel  $\beta$ -sheet secondary structure (1). The intensity of this peak should then also be 10 to 20% of that of a peak at 1,630 to 1,640  $\text{cm}^{-1}$ , which is the case here. The ratio between integrals of the 1,640  $\text{cm}^{-1}$  absorption and the sum of the 1,640 and 1,665  $\text{cm}^{-1}$  absorptions is 44%, which may represent an approximate estimate of the  $\beta$ -sheet content. The spectrum is very similar to that observed for oligomers of wild-type  $A\beta_{42}$  (2).

1. Chirgadze YN, Nevskaya NA (1976) Infrared spectra and resonance interaction of amide-I vibration of the antiparallel-chain pleated sheet. *Biopolymers* 15:607–625.
2. Cerf E, et al. (2009) Antiparallel  $\beta$ -sheet: A signature structure of the oligomeric amyloid  $\beta$ -peptide. *Biochem J* 421:415–423.

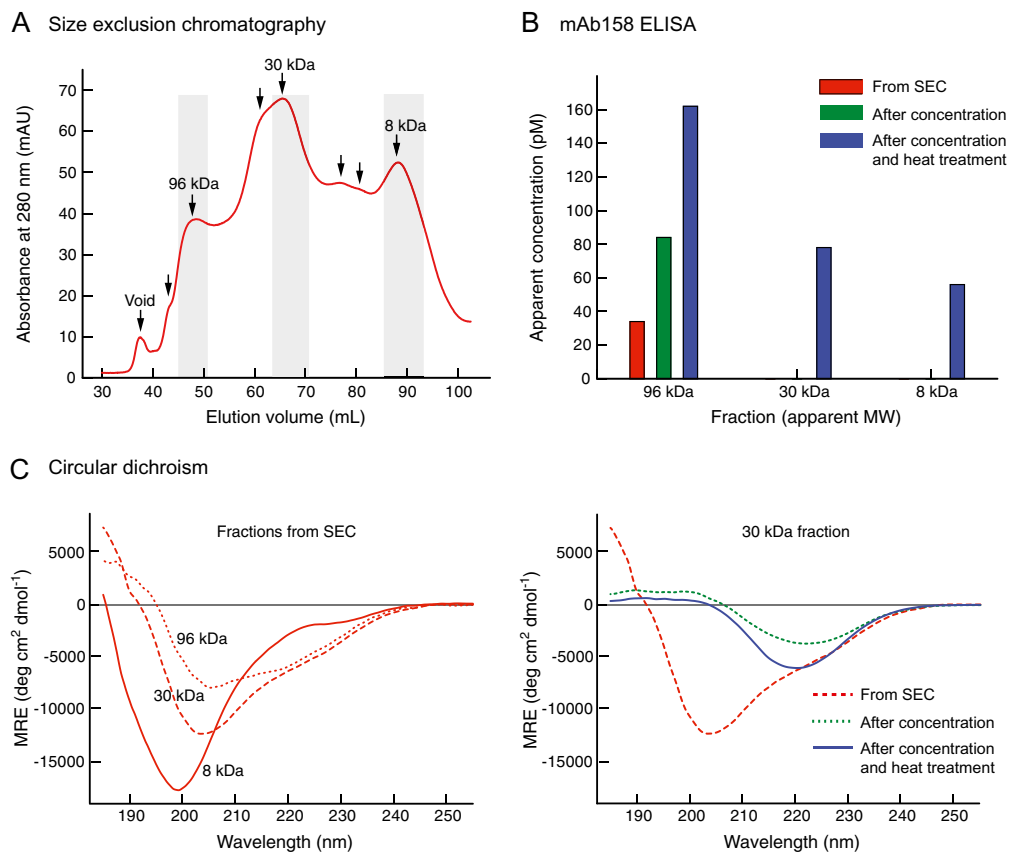


**Fig. 54.**  $A\beta_{40CC}$  monomer and low-molecular weight (LMW) oligomers can be transformed into mAb158 binding  $\beta$ -sheet oligomers by concentration and heat treatment. The figure shows results also shown in Fig. 2 *B* and *C*, with additional CD and mAb158 ELISA analyses. (*A*) Size exclusion chromatography on a Superdex 75 PG 16/60 column. Monomeric  $A\beta_{40CC}$  was loaded in 7-M GdmCl denaturant and eluted with native phosphate buffer. Arrows indicate elution of oligomeric aggregates and remaining monomeric species (8 kDa). The column was calibrated to  $V_E = -37.1 \cdot \log(MW) + 232.2$ , where  $V_E$  is the elution volume of globular molecular weight standards. The shading indicates pooling of SEC fractions for further characterization. Sample amount:  $\sim 3$  mg. (*B*) mAb158 ELISA of three fractions separated by SEC and the same fractions after concentration ( $\sim 0.6$  mM), and after concentration and heat treatment (10 min at  $60^\circ\text{C}$ ). Only heat-treatment results in the detection of the 8- and 30-kDa samples. The heat-induced  $A\beta_{40CC}$   $\beta$ -sheet oligomers/protofibrils remain stable when diluted to 130 pM used in the ELISA. Measured optical densities were converted to apparent concentrations using a standard curve for protofibrillar wild-type  $A\beta_{42}$ . (*C*) CD (mean residue ellipticity) of SEC fractions of different molecular weight (*Left*) and of the 30-kDa fraction from SEC, after concentration, and after concentration and heat treatment (*Right*). CD was measured at the concentrations obtained in SEC fractions (8–16  $\mu\text{M}$ ) or in a 0.1-mm cell without dilution of concentrated samples. Buffer: 50 mM sodium phosphate, 50 mM NaF at pH 7.2.

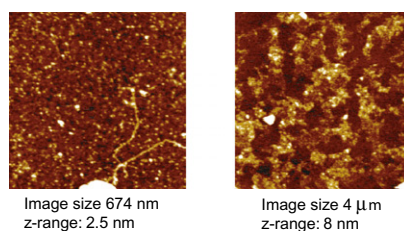


**Fig. 55.** AFM shows that A11 antibody binding HMW SEC fractions of  $A\beta_{42CC}$  are heterogeneous and contain long protofibrils and large amorphous aggregates. Images were acquired in intermittent contact mode on a mica substrate in air. The HMW fractions bind both the A11 antibody and the mAb158 antibody. SEC fractions containing LMW protofibrils and  $\beta$ -sheet oligomers are recognized by mAb158 antibody, but not by A11, indicating that it is the larger aggregates in the AFM picture to the right that bind A11. See also Fig. 56.

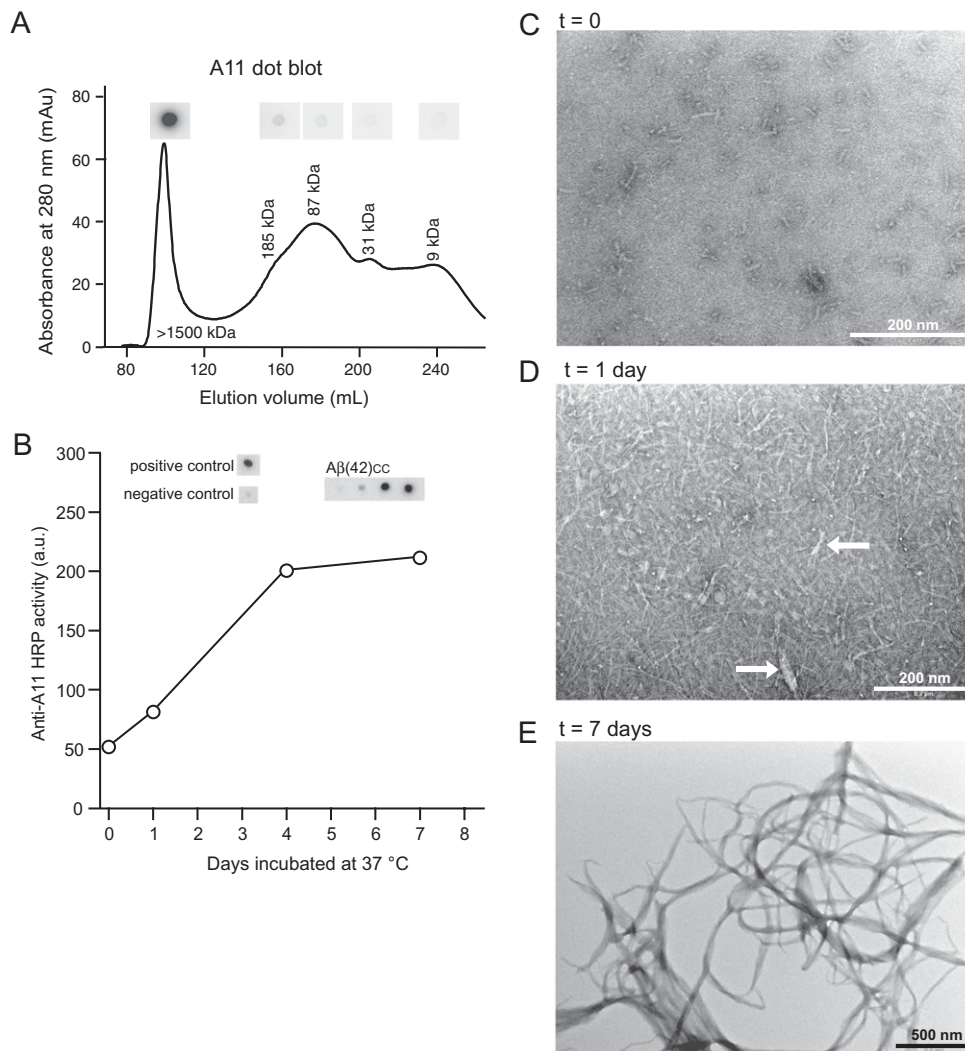


**Fig. S6.** Aging of  $A\beta_{42cc}$  LMW oligomers at 37 °C results in the formation of large nonfibrillar A11 binding aggregates. (A) A11 antibody dot-blot analysis of  $A\beta_{42cc}$  aggregates separated by SEC on a Sephacryl 300 HR 26/60 column. Results from blotting are displayed above the analyzed SEC fractions. Peptide concentrations were equalized before blotting. (B) A11 dot blots of  $A\beta_{42cc}$  LMW oligomers stored at 37 °C. The A11 epitope appears within days. (The dot-blot image at the upper right is the same as in Fig 3D.) (C–E) Time dependence of aggregation monitored by TEM. (D) Arrows indicate the large and 19- to 25-nm wide aggregates that appear simultaneously with A11 binding. Smaller thread-like aggregates have a diameter of 6 nm and vary in length, suggesting that they are long protofibrils. (E) After 1 wk the sample appears to consist of only very large nonamyloid aggregates, but the A11 epitope remains in these.